Micron 115 (2018) 54–63

Contents lists available at ScienceDirect

Micron

journal homepage: www.elsevier.com/locate/micron

In situ oxidation and reduction of cerium dioxide nanoparticles studied by scanning transmission electron microscopy

Aaron C. Johnston-Peck[a,*], Wei-Chang D. Yang[b,c], Jonathan P. Winterstein[b], Renu Sharma[b], Andrew A. Herzing[a,*]

[a] Material Measurement Laboratory, National Institute of Standards and Technology, Gaithersburg, MD 20899, USA
[b] Center for Nanoscience and Technology, National Institute of Standards and Technology, Gaithersburg, MD 20899, USA
[c] Maryland NanoCenter University of Maryland College Park, MD 20742, USA

ARTICLE INFO

Keywords:
Cerium dioxide
Oxidation
Reduction
Scanning transmission electron microscopy

ABSTRACT

Cerium dioxide nanocubes and truncated octahedra were reduced and oxidized in the scanning transmission electron microscope. The reduction process was stimulated by the electron beam and oxidation was supported by background gases in the microscope environment. High-angle annular dark field imaging is sensitive to local lattice distortions that arise as oxygen vacancies are created and cerium cations reduce enabling high spatial resolution characterization of this process with temporal resolution on the order of seconds. Such measurements enable us to differentiate and infer that the observed behavior between the nanocubes and truncated octahedra may be due to the difference in crystallographic termination of surfaces. In situ measurements taken with different partial pressures of oxygen reveal the cerium oxidation state and the dose rate threshold for the onset of beam reduction are influenced by the environment. Increasing oxygen partial pressure reduces the Ce^{3+} content and decreases susceptibility to electron beam driven reduction.

1. Introduction

In situ scanning transmission electron microscopy (STEM) offers the opportunity to observe materials under dynamic conditions with high spatial resolution. Here we observe the oxidation and reduction of cerium dioxide (CeO_2, ceria) nanoparticles using STEM and electron energy loss spectroscopy (EELS). CeO_2 is reduced by highly-energetic electron beams.(Garvie and Buseck, 1999) This behavior has been demonstrated to occur when the beam current is increased above a critical dose-rate threshold (Johnston-Peck et al., 2016a). Upon decreasing the beam current, the reduced nanoparticle begins to oxidize through interactions with the background gases in the microscope environment. To study this transformation requires both adequate spatial and temporal resolution. STEM-EELS spectrum imaging has produced datasets quantifying the oxidation state of cerium cations in ceria with atomic spatial resolution (Turner et al., 2011). Unfortunately the dwell time in a spectrum image is typically on the order of milliseconds compared to microseconds for a bright field or annular dark field (ADF)-STEM image. This means the temporal resolution of spectrum imaging is worse for a given set of sampling conditions and would face limitations in tracking dynamic processes. One method to circumvent this limitation is to extract additional information related to the reduction-oxidation (redox) process directly from the ADF images to supplement the EELS data.

To this point, when the sample is oriented to a high-symmetry-crystallographic axis, electron channeling becomes pronounced and local changes in the sample can manifest as contrast within the resulting ADF images. In CeO_2 specifically, atomic static displacements due to oxygen vacancies and the different ionic radius of Ce^{3+} and Ce^{4+} cations will generate contrast (Johnston-Peck et al., 2016b). The relative simplicity of a single-crystal nanomaterial, without additional features (e.g., line or planar defects) that can also be sources of contrast, presents a situation where the image contrast can be interpreted beyond the mass-thickness relationship of high-angle annular dark field STEM (HAADF-STEM) images to being qualitatively sensitive to relative differences in the extent of reduction. Therefore, in addition to being able to identify different crystallographic phases, we can also discriminate between materials that are the same phase but are anion-deficient (i.e., fluorite CeO_2 and fluorite CeO_{2-x}). This enables tracking of the conversion from CeO_2 to Ce_2O_3 and then back to CeO_2 with a combined temporal and spatial resolution that a spectroscopic technique alone (e.g., STEM-EELS) is currently unable to provide.

* Corresponding authors at: Material Measurement Laboratory, National Institute of Standards and Technology, 100 Bureau Drive Mailstop 8372, Gaithersburg, MD 20899, USA.
E-mail addresses: aaron.johnston-peck@nist.gov (A.C. Johnston-Peck), andrew.herzing@nist.gov (A.A. Herzing).

https://doi.org/10.1016/j.micron.2018.08.008
Received 8 June 2018; Received in revised form 23 August 2018; Accepted 24 August 2018
Available online 30 August 2018
0968-4328/ Published by Elsevier Ltd.

With HAADF-STEM imaging we observe nucleation and growth of the cubic sesquioxide phase (C-Ce_2O_3) in nanocubes, as well as the spatial dependence of the oxidation process in nanocubes and truncated octahedra to CeO_2 from CeO_{2-x}. Analyzing this information along with EELS data we correlate differences in redox activity between particle geometries as a function of surface termination. To appreciate the influence of environment on CeO_2 and the role it plays on the measurement process we measure the critical-dose rate threshold necessary to reduce CeO_2 and quantify Ce^{3+} content as a function of gas pressure using environmental STEM (ESTEM). We observe increasing oxygen pressure affects the results by increasing the critical-dose rate threshold. Also, the Ce^{3+} content of ≈ 5 nm nanoparticles were found to be responsive to environment suggesting that the changes in oxygen chemical potential can influence the outcome of measurements made in the electron microscope.

2. Materials and methods

Image and EELS data shown in Figs. 1–6 and 8a was recorded on an FEI Titan 80–300 equipped with a spherical-aberration corrector for the probe-forming lens. The microscope was operated at an accelerating voltage of 300 kV. The probe convergence angle was ≈ 13.5 mrad; HAADF-STEM images were acquired with collection angles of ≈ (88–175) mrad or ≈ (112–168) mrad. CeO_2 nanocubes were synthesized using wet chemical methods, details can be found in previous reports (Johnston-Peck et al., 2016a,b). CeO_2 truncated octahedron and nanoparticles were acquired from Sigma-Aldrich and Strem Chemicals, respectively. Samples were deposited onto a carbon support film and plasma cleaned by a low energy RF plasma (Ar/O_2) to prevent the build-up of amorphous carbon during electron beam irradiation, as a carbon shell inhibits reduction of the CeO_2 particles (Johnston-Peck et al., 2016a).

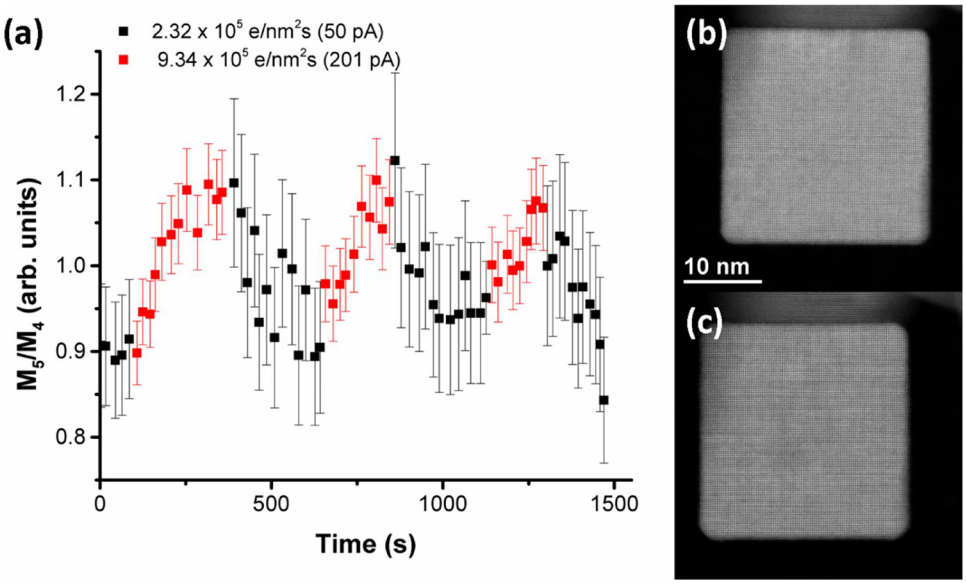

Fig. 1. The ratio of the Ce $M_{4,5}$ peaks as a function of time as the dose rate was changed. Increases in the M_5/M_4 ratio reflect an increased Ce^{3+} concentration. When the dose rate is above the critical-dose rate threshold (red points) the particle reduces, conversely when the dose rate is below the critical-dose rate threshold (black points) the particle oxidizes. HAADF-STEM images of the particle before (b) and after (c) the exposure experiment in (a). (For interpretation of the references to colour in this figure legend, the reader is referred to the web version of this article).

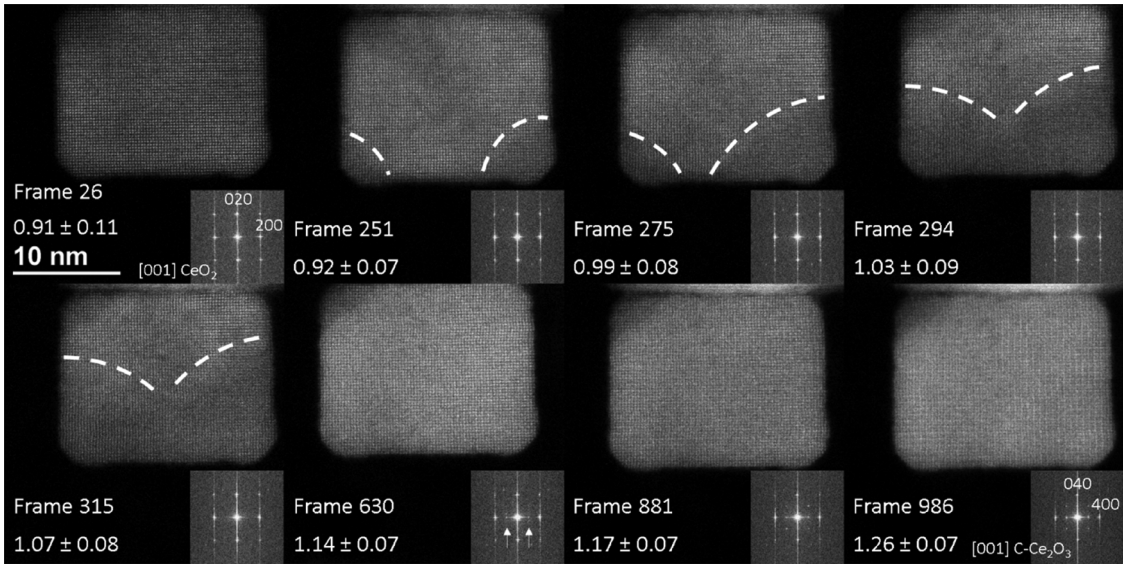

Fig. 2. A series of HAADF-STEM images with FFT of a CeO_2 nanocube being reduced to C-Ce_2O_3. As CeO_{2-x} forms contrasting regions can be observed in Frames 251, 275, 294, and 315 and are marked with dashed lines. In Frame 630 the onset of oxygen vacancy ordering is observed and C-Ce_2O_3 begins forming, arrows in the FFT indicate the presence of new reflections associated with the phase change to C-Ce_2O_3. Ce $M_{,5}$ white-line ratio EELS measurements reported in the bottom left-hand corner, correlate the change in image contrast to a change in cerium oxidation state. Dose rates: Frame 26 – 3.24 * 10^5 e·nm^{-2}·s^{-1}; Frame 251, 275, 294, 315 – 5.56 * 10^5 e·nm^{-2}·s^{-1}; Frame 630 – 9.26 * 10^5 e·nm^{-2}·s^{-1}; Frame 881, 986 – 1.11 * 10^6 e·nm^{-2}·s^{-1}. The vertical streaking in the FFTs is due to scan noise.